Progress in Nonlinear Dynamics and Chaos
Vol. 2, No. 2, 2014, 51-60
ISSN: 2321 – 9238 *(online)*
Published on 26 December 2014
www.researchmathsci.org

MHD Couette Flow of a Casson Fluid Between Parallel Porous Plates

***M. Wahiduzzaman**[*1], **Md. Tajul Islam**[2], **Parvin Sultana**[3] **and M. Afikuzzaman**[4]*
[1,3,4]Mathematics Discipline, Khulna University, Khulna-9208, Bangladesh
[2]Begum Rokeya University, Rangpur, Bangladesh
[*]Corresponding author's email: wahidmathku@gmail.com

Received 29 October 2014; accepted 21 November 2014

Abstract. The unsteady magneto hydrodynamic flow of an electrically conducting viscous incompressible non-Newtonian Casson fluid bounded by two parallel non-conducting porous plates with porous medium in studied with heat transfer considering the Hall effect. An external uniform magnetic field is applied perpendicular to the plates and the fluid motion is subjected to a uniform section and injection. The lower plate is stationary and the upper plate is suddenly set into motion and simultaneously suddenly isothermally heated to a temperature other than the lower plate temperature. At first the system of equations have transformed by usual transformation into a non-dimensional form. After that, the non-similar partial differential equations have solved numerically by Crank-Nicolson implicit finite difference. The results of this study have discussed for the different values of the well-known parameters with different time step.

Keywords: MHD, Casson fluid, implicit finite difference

1. Introduction

Casson fluid is a shear thinning liquid which has an infinite viscosity at a zero rate of shear, a yield stress below which no flow occurs and a zero viscosity at an infinite rate of shear. Casson's constitute equation represents a nonlinear relationship between stress and rate of strain and has been found to be accurately applicable to silicon suspensions, suspensions of bentonite in water and lithographic varnishes used for printing inks. Attia et al. [1] has studied the influence of the Hall current on the velocity and temperature fields of an unsteady Hartmann flow of a conducting Newtonian fluid between two infinite non-conducting horizontal parallel and porous plates. Several works on MHD are in [2-4]. Attia et al. [5] studied the transient MHD Couette flow of a Casson fuuid between parallel plates with heat transfer. The extension of such problem to the case of Couettee flow of non-Newtonian Casson fluid is done in the present study for porous medium. The upper plate is moving with a uniform velocity while the lower plate is stationary. The fluid is acted upon by a constant pressure gradient, a uniform suction from above, and a uniform injection from below and is subjected to a uniform magnetic field perpendicular to the plates. The two plates are kept at two different but constant temperatures. This configuration is a good approximation of some practical situations such as heat exchangers, flow meters, and pipes that connect system components.

2. Formulation of the problem

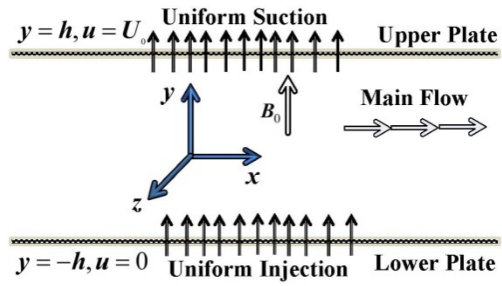

Figure : Physical configuration of the Problem

The fluid is assumed to be laminar, incompressible and obeying a Casson model and flows between two infinite horizontal plates located at the $y = \pm h$ planes. The upper plate is suddenly set into motion and moves with a uniform velocity U_0 while the lower plate is stationary. The upper plate is simultaneously subjected to asset change in temperature from T_1 to T_2. Then, the upper and lower plates are kept constant temperature T_2 and T_1 respectively, with $T_2 > T_1$. The fluid is acted upon by a constant pressure gradient $\frac{dp}{dx}$ in the x -direction and a uniform suction from above and injection from below which are applied at $t = 0$. A uniform magnetic field B_0 is applied in the positive y -direction and is assumed undistributed as the induced magnetic field is neglected by assuming a very small magnetic Reynolds number.

The flow of the fluid is governed by the momentum equation

$$\rho \frac{Dv}{Dt} = \nabla.(\mu \nabla v) - \nabla p + J \times B_0 \tag{1}$$

where ρ is the density of the fluid and μ is the apparent viscosity of the model and is given by

$$\mu = \left[K_c + \left(\tau_0 \Big/ \sqrt{(\frac{\partial u}{\partial y})^2 + (\frac{\partial u}{\partial y})^2)} \right)^{1/2} \right]^2 \tag{2}$$

where ${K_c}^2$ is the Casson's coefficient of viscosity and τ_0 is the yield stress. If the Hall term is retained, the current density J is given by; $J = \sigma \left[v \times B_0 - \beta \left(J \times V_0 \right) \right]$ (3)

where σ is the electric conductivity of the fluid and β is the Hall factor.

Equation (3) may be solved in J to yield;

$$J \times B_0 = -\frac{\sigma {B_0}^2}{1 + m^2} \left[\left(u + mw \right) \; i + \left(w - mu \right) \; k \right] \tag{4}$$

where, m is the Hall parameter and $m = \sigma \, \beta \, B_0$.

Thus two component of the momentum Equations are:

$$\rho \frac{\partial u}{\partial t} + \rho v_0 \frac{\partial u}{\partial y} = -\frac{\partial p}{\partial x} + \frac{\partial}{\partial t}\left(\mu \frac{\partial u}{\partial y} \right) - \frac{\sigma B_0^{\;2}}{1+m^2}\left[\left(u + mw \right) \right] - \frac{\rho \gamma}{k} u \tag{5}$$

$$\rho \frac{\partial w}{\partial t} + \rho v_0 \frac{\partial w}{\partial y} = \frac{\partial}{\partial y}\left(\mu \frac{\partial w}{\partial y} \right) - \frac{\sigma B_0^{\;2}}{1+m^2}\left[\left(w - mu \right) \right] - \frac{\rho \gamma}{\mathrm{k}} w \tag{6}$$

The energy equation with viscous and Joule dissipations is given by

$$\rho c_p \frac{\partial T}{\partial t} + \rho c_p v \frac{\partial T}{\partial y} + = k \frac{\partial^2 T}{\partial y^2} + u \left[\left(\frac{\partial u}{\partial y} \right)^2 + \left(\frac{\partial w}{\partial y} \right)^2 \right] + \frac{\sigma B_0^2}{\left(1+m^2 \right)} \left(u^2 + w^2 \right) \tag{7}$$

where C_p and k are respectively the specific heat capacity and the thermal conductivity of the field.

The initial and boundary conditions of the problem are given by

$u = w = 0$ at $t < 0$, and $w = 0$ at $y = -h$ and $y = h$ for $t > 0$ (8)

$u = 0$ at $y = -h$ for $t \le 0$, $u = U_\circ$ at $y = h$ for $t > 0$, (9)

$T = T_1$ at $t \le 0$, $T = T_2$ at $y = h$ and $T = T_1$ at $y = -h$ for $t > 0$ (10)

Introducing the following non-dimensional quantities;

$$\bar{x} = \frac{x}{h}, \quad \bar{y} = \frac{y}{h}, \quad \bar{t} = \frac{tU_0}{h}, \quad \bar{u} = \frac{u}{U_0}, \quad \bar{\omega} = \frac{\omega}{U_0}, \quad \bar{p} = \frac{p}{\rho U_O^2}, \quad \theta = \frac{T - T_1}{T_2 - T_1}, \quad \bar{\mu} = \frac{\mu}{K_c^2}$$

Now for equations (5)-(10), we get after dropping hates;

$$\frac{\partial u}{\partial t} + \frac{S}{R_e}\frac{\partial u}{\partial y} = -\frac{dp}{dx} + \frac{1}{R_e}\left[\frac{\partial}{\partial y}\left(\mu \frac{\partial u}{\partial y} \right) - \frac{H_a^{\;2}}{1+m^2}\left(u + mw \right) \right] - \gamma u \tag{11}$$

$$\frac{\partial w}{\partial t} + \frac{S}{R_e}\frac{\partial w}{\partial y} = \frac{1}{R_e}\left[\frac{\partial}{\partial y}\left(\mu \frac{\partial w}{\partial \bar{y}} \right) - \frac{H_a^{\;2}}{1+m^2}\left(w - mu \right) \right] - \gamma w \tag{12}$$

$$\frac{\partial \theta}{\partial t} + \frac{S}{R_e}\frac{\partial \theta}{\partial y} = \frac{1}{P_r}\frac{\partial^2 \theta}{\partial y^2} + E_c \mu \left[\left(\frac{\partial u}{\partial y} \right)^2 + \left(\frac{\partial w}{\partial y} \right)^2 \right] + \frac{H_a^{\;2} E_c}{1+m^2}\left(u^2 + w^2 \right) \tag{13}$$

$u = w = 0$ for $t \le 0$ and $u = w = 0$ at $y =$ -1 (14)

$w = 0$, $u = 1$, at $y = 1$ for $t > 0$,

$\theta = 0$ for $t \le 0$ and $\theta = 0$ at $y = -1$, $\theta = 1$ at $y = 1$ for $t > 0$ (15)

The shear stress at the two walls is given by

$$\tau_D = \left[\left(\left(\frac{\partial u}{\partial y} \right)^2 + \left(\frac{\partial w}{\partial y} \right)^2 \right)^{1/4} + \frac{\tau_D^{1/2}}{\left(\left(\frac{\partial u}{\partial y} \right)^2 + \left(\frac{\partial w}{\partial y} \right)^2 \right)^{1/4}} \right] = \pm 1 \text{ and } \mu = \left[1 + \left(\frac{\tau_{\mathrm{D}}}{\sqrt{\left(\frac{\partial u}{\partial y} \right)^2 + \left(\frac{\partial w}{\partial y} \right)^2}} \right)^{1/2} \right] \tag{16}$$

where, τ_D (dimensionless yield stress) $= \dfrac{\tau_0 h}{K_c^2 U_0}$ (Casson number)

$S = \dfrac{\rho v_0 h}{K_c^2}$ (suction parameter), $P_r = \dfrac{\rho c_p U_0 h}{k}$ (prandtl number),

$E_c = \dfrac{U_0 K_c^2}{\rho c_p h(T_2 - T_1)}$ (Eckert number), ${H_a}^2 = \dfrac{\sigma B_0^2 h^2}{K_c^2}$ (Hartmann number squared)

3. Numerical solution

Equations (11)-(13) represent couple system of non-linear partial differential equations which are solved numerically under the initial and boundary conditions (14)-(15) using the Crank-Nicolson implicit method [6]. An iterative scheme is used to solve the liberalized system of difference equations. The solution at a certain time step is chosen as an initial guess for next time step and the iterative are continued till convergence, within a prescribed accuracy. Finally, the resulting block tridiagonal system is solved using the generalized Thomas-algorithm.

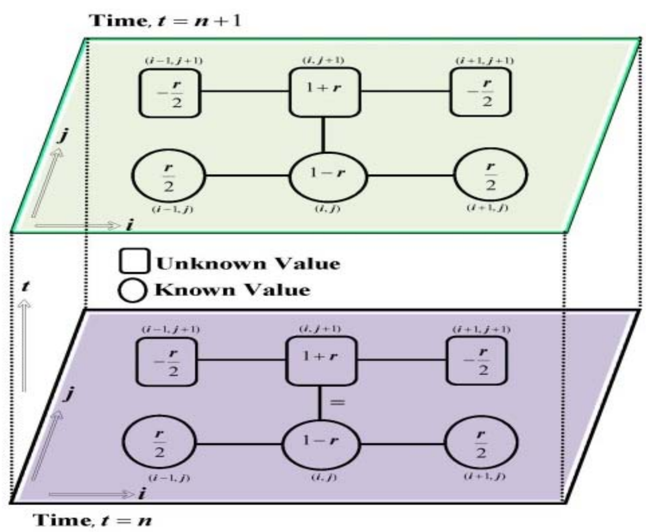

Figure: Implicit finite difference grid space

The value of the velocity components are substituted in the right hand side of Equation (13) which is solved numerically with the initial and boundary conditions (14)-(15) using central. Finite difference equation relating the variables are obtained by writing the equations the mid-point of the computational cell and then replacing the different terms by their second order central difference approximations in the y -direction. The diffusion terms are replaced by the average of the central differences at two successive time-levels. The computational domain is divided into meshes each of dimensions Δt and Δy in time and space respectively.

$$\frac{\partial u}{\partial t}=\frac{U_{i,j}^{n+1}-U_{i,j}^{n}}{\Delta t},\ \frac{\partial u}{\partial y}=\frac{U_{i,j+1}^{n+1}-U_{i,j-1}^{n+1}+U_{i,j+1}^{n}-U_{i,j-1}^{n}}{4\Delta y}$$

$$\frac{\partial^2 u}{\partial y^2}=\frac{U_{i,j-1}^{n+1}-2U_{i,j}^{n+1}+U_{i,j+1}^{n+1}-U_{i,j-1}^{n}-2U_{i,j}^{n}+U_{i,j+1}^{n}}{2(\Delta y)^2},\ U=\frac{U_{i,j}^{n+1}+U_{i,j}^{n}}{2},\ \frac{\partial w}{\partial t}=\frac{W_{i,j}^{n+1}-W_{i,j}^{n}}{\Delta t}$$

$$\frac{\partial w}{\partial y}=\frac{W_{i,j+1}^{n+1}-W_{i,j-1}^{n+1}+W_{i,j+1}^{n}-W_{i,j-1}^{n}}{4\Delta y},\ \frac{\partial^2 w}{\partial y^2}=\frac{W_{i,j-1}^{n+1}-2W_{i,j}^{n+1}+W_{i,j+1}^{n+1}-W_{i,j-1}^{n}-2W_{i,j}^{n}+W_{i,j+1}^{n}}{2(\Delta y)^2}$$

$$W=\frac{W_{i,j}^{n+1}+W_{i,j}^{n}}{2},\ \frac{\partial \theta}{\partial t}=\frac{\theta_{i,j}^{n+1}-\theta_{i,j}^{n}}{\Delta t},\ \frac{\partial \theta}{\partial y}=\frac{\theta_{i,j+1}^{n+1}-\theta_{i,j-1}^{n+1}+\theta_{i,j+1}^{n}-\theta_{i,j-1}^{n}}{4\Delta y}$$

$$\frac{\partial^2 \theta}{\partial y^2}=\frac{\theta_{i,j-1}^{n+1}-2\theta_{i,j}^{n+1}+\theta_{i,j+1}^{n+1}-\theta_{i,j-1}^{n}-2\theta_{i,j}^{n}+\theta_{i,j+1}^{n}}{2(\Delta y)^2}$$

We define the variables $v=u_y$, $\mathrm{B}=\mathrm{w}_{\mathrm{y}}$, $H=\theta_y$ and $\mu'=\mu_y$ to reduce the second order differential Equations (11)-(13) to first order differential equations. The finite difference representations for the resulting first order differential Equations (11) - (13) together the equations defining the new variables take the form;

$$\frac{U_{i,j}^{n+1}-U_{i,j}^{n}}{\Delta t}+\frac{S}{R_e}\left(\frac{U_{i,j+1}^{n+1}-U_{i,j-1}^{n+1}+U_{i,j+1}^{n}-U_{i,j-1}^{n}}{4\Delta y}\right)=-\frac{dp}{dx}+\mu$$

$$\left(\frac{U_{i,j-1}^{n+1}-2U_{i,j}^{n+1}+U_{i,j+1}^{n+1}-U_{i,j-1}^{n}-2U_{i,j}^{n}+U_{i,j+1}^{n}}{2(\Delta y)^2}\right)-\frac{{H_a}^2}{1+m^2}\left(\frac{U_{i,j}^{n+1}+U_{i,j}^{n}}{2R_e}-m\frac{W_{i,j}^{n+1}+W_{i,j}^{n}}{2R_e}\right)-\gamma\left(\frac{U_{i,j}^{n+1}+U_{i,j}^{n}}{2}\right)$$

Again, $\frac{W_{i,j}^{n+1}-W_{i,j}^{n}}{\Delta t}+\frac{S}{R_e}\left(\frac{W_{i,j+1}^{n+1}-W_{i,j-1}^{n+1}+W_{i,j+1}^{n}-W_{i,j-1}^{n}}{4\Delta y}\right)=\mu$

$$\left(\frac{W_{i,j-1}^{n+1}-2W_{i,j}^{n+1}+W_{i,j+1}^{n+1}-W_{i,j-1}^{n}-2W_{i,j}^{n}+W_{i,j+1}^{n}}{2(\Delta y)^2}\right)-\frac{{H_a}^2}{1+m^2}\left(\frac{W_{i,j}^{n+1}+W_{i,j}^{n}}{2R_e}-m\frac{U_{i,j}^{n+1}+U_{i,j}^{n}}{2R_e}\right)-\gamma\left(\frac{W_{i,j}^{n+1}+W_{i,j}^{n}}{2}\right)$$

and $\frac{\theta_{i,j}^{n+1}-\theta_{i,j}^{n}}{\Delta t}+\frac{S}{R_e}\left(\frac{\theta_{i,j+1}^{n+1}-\theta_{i,j-1}^{n+1}+\theta_{i,j+1}^{n}-\theta_{i,j-1}^{n}}{4\Delta y}\right)=$

$$E_c\mu\left[\left(\frac{U_{i,j+1}^{n+1}-U_{i,j-1}^{n+1}+U_{i,j+1}^{n}-U_{i,j-1}^{n}}{4\Delta y}\right)^2+\left(\frac{W_{i,j+1}^{n+1}-W_{i,j-1}^{n+1}+W_{i,j+1}^{n}-W_{i,j-1}^{n}}{4\Delta y}\right)^2\right]$$

$$+\frac{1}{P_r}\left(\frac{\theta_{i,j-1}^{n+1}-2\theta_{i,j}^{n+1}+\theta_{i,j+1}^{n+1}+\theta_{i,j-1}^{n}-2\theta_{i,j}^{n}+\theta_{i,j+1}^{n}}{2\left(\Delta y\right)^2}\right)+\frac{{H_a}^2E_c}{1+m^2}\left[\left(\frac{U_{i,j}^{n+1}+U_{i,j}^{n}}{2}\right)^2+\left(\frac{W_{i,j}^{n+1}+W_{i,j}^{n}}{2}\right)^2\right]$$

Grid-independence studies show that the computational domain $0<t<\infty$ and $-1<y<1$ can be divided into intervals with step sizes $\Delta t=0.001$ and $\Delta y=0.005$ for time and space respectively. Smaller step size does not show any significant change in the results. Convergence of the scheme is assumed when all of the unknowns u, v, w, B, θ and H for the last two approximations differ from unity by less than 10^{-6} for all values of y in $-1 < y < 1$ at every time step. Less than 7 approximations are required to satisfy this convergence criterion for all ranges of the parameters studied here.

4. Results and discussion

To obtain the solutions, the computations have been carried out up to $\tau = 20.00$. The result of the computations show little changes for $\tau = 0.1$ to $\tau = 5.0$ but after $\tau = 5.0$ to $\tau = 20.00$ the result remain approximately same. Thus the solution for $\tau = 20.00$ are essentially steady-state solutions. It has been seen that in case of Couette flow, the pressure gradient term must be constant. Though the most important fluids are atmospheric air, salt water and water so that results are limited to $P_r = 0.71$ (Prandtl number for air at 20^0 c), $P_r = 1.0$ (Prandlt number for salt water at $20^0 c$), $P_r = 7.0$ (Prandtl number for water at $20^0 c$). In addition, the values of other parameter m, S, Ha, E_c and R_e are chosen arbitrary. From figures (1-24), the flow behaviors in the case of coquette flow are represented graphically. Here velocity and temperature distributions with respect to Y are illustrated. Figures (1-3) illustrates that velocity component U, W and temperature θ increases with the increase of R_e. Figure 4 shows that velocity component U decrease with the increase of S. Figure 5 shows that W decreases with the increase of S. Figure 3 exhibits that θ decreases as S increases. Figure 7 shows that velocity component U increases with the increase of H_a. Figure 8 shows that W decreases with the increase of H_a. Figure 9 shows that the temperature distribution has a minor effect for increasing H_a. Figures (10-12) shows that velocity components U, W increase and temperature profiles θ has a minor effect for increasing value of m. Figures (13-14) represent that both the velocity component U and W exhibits a little changes. On the other hand Figure 15 represents that θ decreases with the increases of P_r. Figures(16-17) shows that the velocity distributions has a minor effect for increasing E_c Figure 18 shows that θ increases with the increase of E_c.

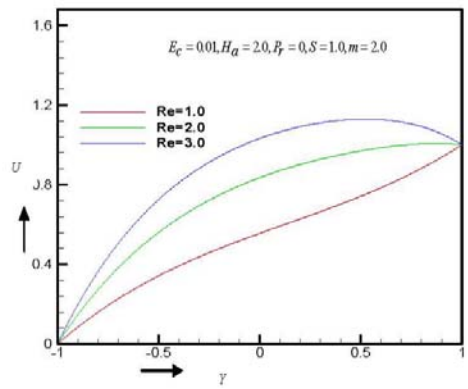

Figure 1: Primary velocity versus Y for different values of Reynolds number at $\tau_D = 5.0$

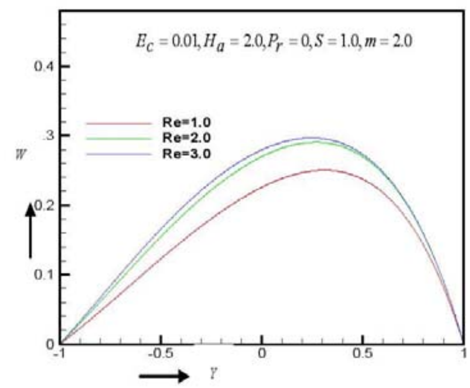

Figure 2: Secondary velocity versus Y for different values of Reynolds number at $\tau_D = 5.0$

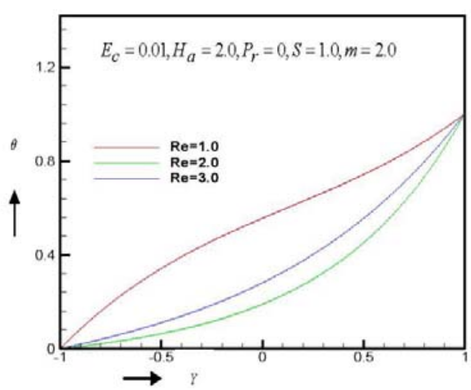

Figure 3: Temperature versus Y for different values of Reynolds number at $\tau_D = 5.0$

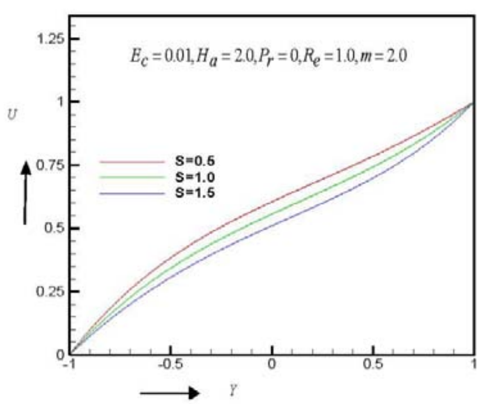

Figure 4: Primary velocity versus Y for different values of Suction parameter at $\tau_D = 5.0$

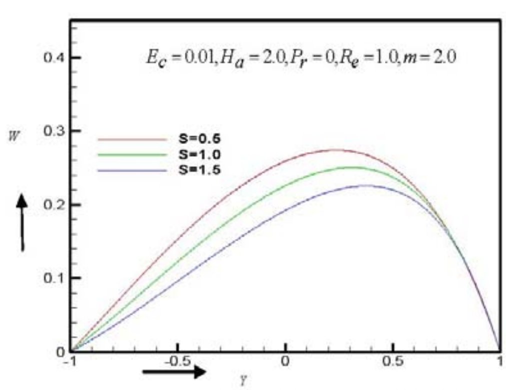

Figure 5: Secondary velocity versus Y for different values of Suction parameter at $\tau_D = 5.0$

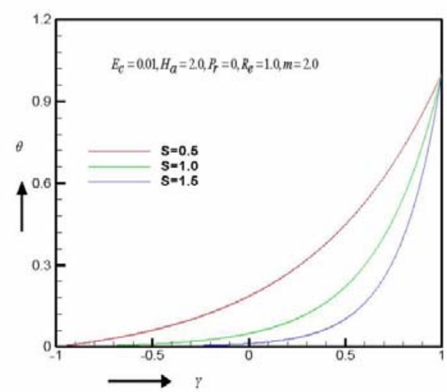

Figure 6: Temperature versus Y for different values of Suction parameter at $\tau_D = 5.0$

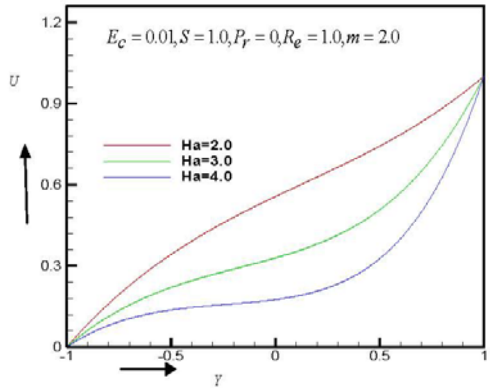

Figure 7: Primary velocity versus Y for different values of Hartmann number at $\tau_D = 5.0$

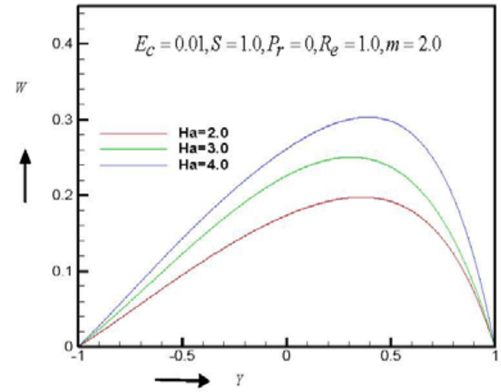

Figure 8: Secondary velocity versus Y for different values of Hartmann number at $\tau_D = 5.0$

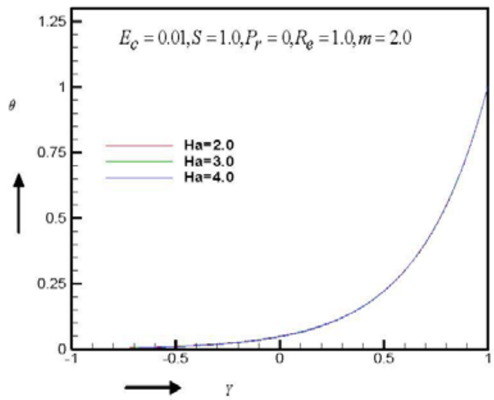

Figure 9: Temperature versus Y for different values of Hartmann number at $\tau_D = 5.0$

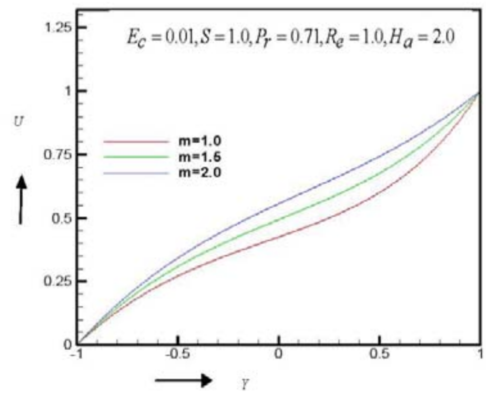

Figure 10: Primary velocity versus Y for different values of Hall parameter at $\tau_D = 5.0$

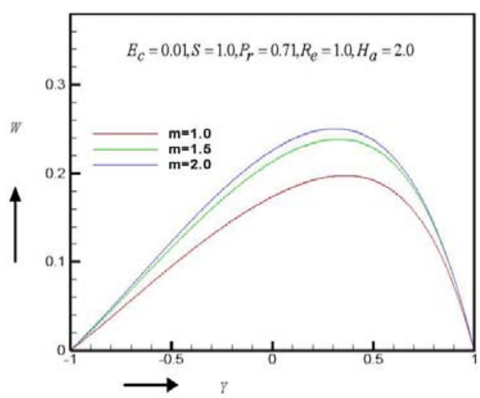

Figure 11: Secondary velocity versus Y for different values of Hall parameter at $\tau_D = 5.0$

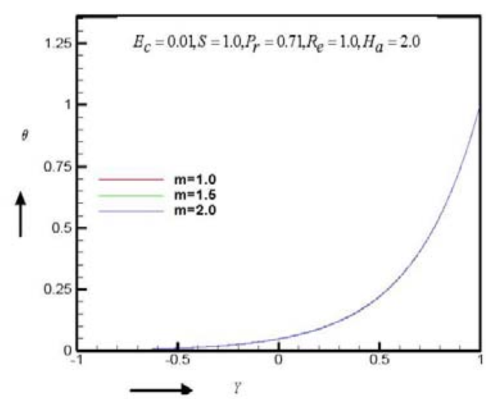

Figure 12: Temperature versus Y for different values of Hall parameter at $\tau_D = 5.0$

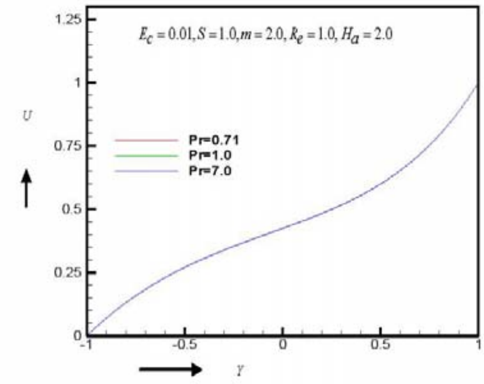

Figure 13: Primary velocity versus Y for different values of Prandlt number at $\tau_D = 5.0$

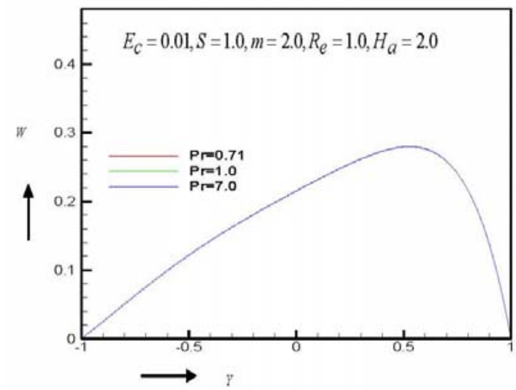

Figure 14: Secondary velocity versus Y for different values of Prandlt number at $\tau_D = 5.0$

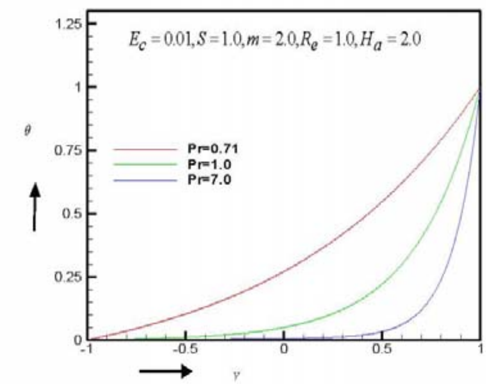

Figure 15: Temperature versus Y for different values of Prandlt number at $\tau_D = 5.0$

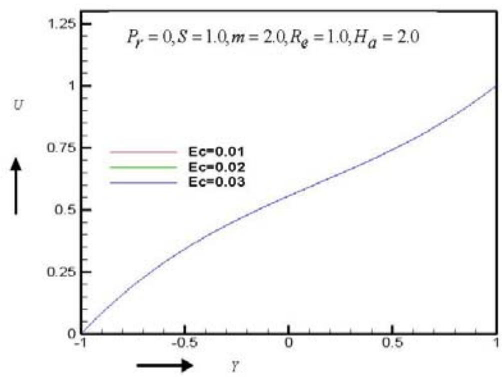

Figure 16: Primary velocity versus Y for different values of Eckert number at $\tau_D = 5.0$

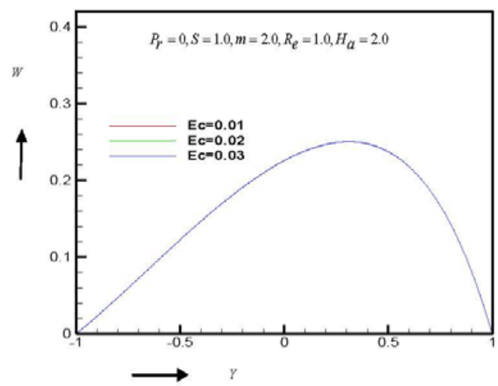

Figure 17: Secondary velocity versus Y for different values of Eckert number at $\tau_D = 5.0$

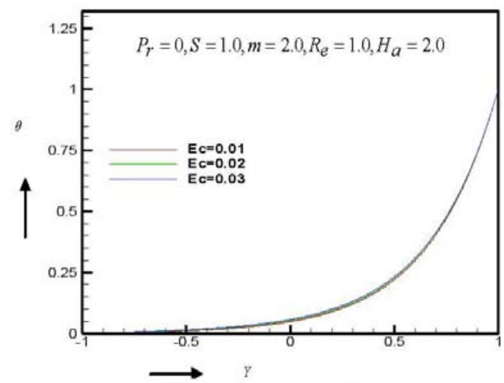

Figure 18: Temperature versus Y for different values of Eckert number at $\tau_D = 5.0$

REFERENCES

1. H.A.Attia and N.A.Kotb, Heat transfer by laminar flow between parallel plates under the consideration of Hall effects, *J. of Aerospace Sci.,* 29 (1962) 286.
2. M.S.Islam, M.Samsuzzoha, S.Ara and P.Dey, MHD free convection and mass transfer flow with heat generation through an inclined plate, *Annals of Pure and Applied Mathematics*, 3(2) (2013) 129-141.
3. M.A.Rahman, M.A.Alim and M.J.Islam, Thermophoresis effect on MHD forced convection on a fluid over a continuous linear stretching sheet in presence of heat generation and power-law wall temperature, *Annals of Pure and Applied Mathematics*, 4(2) (2013) 192-204.
4. M.Hasanuzzaman, B.Mandal and M.M.T.Hossain, A study of similarity solution of unsteady combined free and force convective laminar boundary layer flow about a vertical porous surface with suction and blowing, *Annals of Pure and Applied Mathematics*, 6(1) (2014) 85-97.
5. H.A.Attia and M.E.Sayed Ahmed, Transient MHD couette flow of a casson fluid between parallel plates with heat transfer, *Italian Journal of Pure and Applied Mathematics,* 27 (2010) 19-38.
6. M.Pal, *Numerical Analysis for Scientists and Engineering: Theory and C Programs*, Alpha Science International Limited, Oxford, UK, 2007.